Stress-induced neuron remodeling reveals differential interplay between neurexin and environmental factors

Michael P. Hart[1]

1. Department of Genetics, University of Pennsylvania, Philadelphia PA 19104

ABSTRACT

Neurexins are neuronal adhesion molecules important for synapse maturation, function, and plasticity. While neurexins have been genetically associated with neurodevelopmental disorders including autism spectrum disorders (ASDs) and schizophrenia, they are not deterministic, suggesting that environmental factors, particularly exposures during brain development and maturation, have a significant effect in pathogenesis of these disorders. However, the interplay between environmental exposures, including stress, and alterations in genes associated with ASDs and schizophrenia is still not clearly defined at the cellular or molecular level. The singular *C. elegans* ortholog of human neurexins, *nrx-1*, controls experience-dependent morphologic changes of a GABAergic neuron. Here I show that this GABAergic neuron's morphology is altered in response to each of three environmental stressors (nutritional, proteotoxic, or genotoxic stress) applied during sexual maturation, but not during adulthood. Increased outgrowth of axon-like neurites following prior adolescent stress results from an altered morphologic plasticity that occurs upon entry into adulthood. Despite axonal remodeling being induced by each of the three stressors, only nutritional stress (starvation) impacted behavior and was dependent on neurexin/*nrx-1*. Proteotoxic or genotoxic stress exposure during sexual maturation did not affect behavior despite inducing GABAergic neuron morphologic remodeling that was independent of neurexin/*nrx-1*. The disparate effects of stressors on behavior and their differential reliance on the presence of *nrx-1*, despite impact on GABAergic neuron morphology, is a novel paradigm for understanding how environmental exposures, genetics, and plasticity may contribute to brain dysfunction in ASDs and schizophrenia.

INTRODUCTION

Autism spectrum disorders (ASDs) and schizophrenia are neurodevelopmental/neuropsychiatric disorders characterized by social and cognitive phenotypes that can be extremely heterogeneous in makeup and severity. Their complex etiology is a consequence of both genetic and environmental risk factors likely playing pathogenic roles (Cattane, Richetto, & Cattaneo, 2018; Chaste & Leboyer, 2012; Hallmayer et al., 2011; Hertz-Picciotto, Schmidt, & Krakowiak, 2018; Sandin et al., 2014; Schmitt, Malchow, Hasan, & Falkai, 2014; Tick, Bolton, Happe, Rutter, & Rijsdijk, 2016). Exposure to stress is a risk factor for ASDs and schizophrenia, and may influence the course of these disorders (Bishop-Fitzpatrick, Mazefsky, Minshew, & Eack, 2015; Fuld, 2018; Schmitt et al., 2014). Recent work on the genetics of ASDs and schizophrenia has implicated numerous genes involved in overlapping pathways, including many neuronal/synaptic genes, to be associated with both disorders (Autism Spectrum Disorders Working Group of The Psychiatric Genomics, 2017; Waltereit, Banaschewski, Meyer-Lindenberg, & Poustka, 2014). However, the seemingly important interplay between environmental exposures, including stress, and variants in genes associated with ASDs and schizophrenia is still not clearly defined.

Stress exposure has many impacts on the brain that could explain the connection between stress and neurodevelopmental disorders. The morphology of a neuron, especially of its dendrites and axons, mediates neuron and circuit function by dictating its connectivity potential. Over a decade of work has characterized the impact of stress on neurons morphology in the vertebrate brain, specifically with regard to atrophy and/or hypertrophy of excitatory dendrites in the hippocampus, amygdala, and cortex in response to stress (Cook & Wellman, 2004; McEwen, Nasca, & Gray, 2016; Vyas, Mitra, Shankaranarayana Rao, & Chattarji, 2002). Recent work has also identified stress-induced dendritic remodeling in GABAergic inhibitory interneurons in the same brain regions, in some cases mirroring the direction of dendrite remodeling of excitatory neurons (Gilabert-Juan, Bueno-Fernandez, Castillo-Gomez, & Nacher, 2017; Gilabert-Juan, Castillo-Gomez, Guirado, Molto, & Nacher, 2013; Gilabert-Juan, Castillo-Gomez, Perez-Rando, Molto, & Nacher, 2011). The interplay between excitatory and inhibitory remodeling is of particular interest in neurodevelopmental disorders given the popular

hypothesis that an imbalance between excitatory and inhibitory signaling in the brain is involved in the pathogenesis of these disorders (Jiang, Cowell, & Nakazawa, 2013; Schmitt, Hasan, Gruber, & Falkai, 2011; Yizhar et al., 2011).

Studies have tried to connect stress-induced changes in neuron morphology with changes in the functional output of neurons, namely relevant behavioral changes. While stress-induced dendritic hypertrophy of neurons in the rodent hippocampus have been shown to correlate with changes in spatial learning tasks, some studies have demonstrated that behavioral changes following stress can be separated from neuron remodeling events (Conrad, 2006; Conrad, LeDoux, Magarinos, & McEwen, 1999; Conrad, Ortiz, & Judd, 2017; Vyas et al., 2002). Thus, a direct connection between stress-induced dendritic remodeling and behavior has been difficult to fully define. The majority of vertebrate studies also lack the temporal resolution to analyze the dynamics of neuron morphologic changes following stress, and while the mechanisms controlling excitatory dendrite remodeling in response to stress have been studied (McEwen et al., 2016), those controlling remodeling in inhibitory neurons, or the interplay between excitatory and inhibitory remodeling, are still relatively unknown. Lastly, although stress seems to alter the presynaptic dynamics of inhibitory neurons (Czeh et al., 2018; McKlveen et al., 2016), *in vivo* studies of axon remodeling in response to stress are lacking, in large part due to the technical difficulty of performing such studies in the vertebrate brain.

C. elegans has been utilized as a powerful and simple model for neuronal response to stress, including various environmental, internal/developmental, and aging stressors (Kagias, Nehammer, & Pocock, 2012). We recently described experience-dependent morphologic plasticity in the nematode *C. elegans*, where the GABAergic DVB neuron undergoes progressive experience-dependent outgrowth of axon-like neurites in adult males. This plasticity alters circuit connectivity to cause changes in male mating and defecation behaviors (Hart & Hobert, 2018). We identified the singular *C. elegans* ortholog of human neurexins, *nrx-1*, to be required in the DVB neuron for this neurite outgrowth. Neurexins are synaptic adhesion molecules with diverse functions in synaptic formation, maturation, maintenance, function, and plasticity (Sudhof, 2017), and have been genetically associated with both ASDs and

schizophrenia (Gauthier et al., 2011; Kirov et al., 2009; Reichelt, Rodgers, & Clapcote, 2012). Therefore, neurexins are strong candidates for mediating changes in neuron morphology and behavior in response to environmental stress.

This *C. elegans* model of GABAergic morphologic plasticity provides a platform to investigate the impact of stress on GABAergic axonal morphology, including the temporal dynamics of morphologic plasticity. My results demonstrate that stress, specifically during sexual maturation of the male nervous system (fourth larval stage, 'adolescence' (Snoek et al., 2014)), alters the morphology of the DVB GABAergic neuron, with outgrowth of axon-like neurites becoming more elaborate in early adulthood. Each of three distinct stressors impact GABAergic neuron morphology, resulting in lasting morphologic changes. Despite this, each stressor differentially impacts downstream functional output and behavior with disparate dependence on *nrx-1*. These findings demonstrate that stress also alters axonal morphology and morphologic dynamics in GABAergic neurons. This work provides an example of an underlying genetic defect (*nrx-1* mutation) resulting in distinct neuronal and behavioral responses to different environmental stressors, providing a platform for understanding the combinatorial impact of genetics and environment on risk of pathogenesis of neuropsychiatric disorders.

RESULTS

Adolescent stress alters GABAergic neuron morphology by altering morphologic plasticity in adulthood

The GABAergic DVB neuron is present in both male and hermaphrodite *C. elegans*, but undergoes experience-dependent morphological plasticity only in males (Hart & Hobert, 2018). In studying morphologic plasticity of the GABAergic DVB neuron in adult male *C. elegans* (**Fig.1A**), I noted that dietary history (food vs. no food) appeared to affect DVB neurite outgrowth. To confirm this observation, I compared DVB neurite outgrowth between well-fed males and males cultivated without food for 18 hours beginning in the mid-L4 stage (**Fig.1B**). DVB in males 'starved' for 18 hours had increased total neurite length and neurite junctions compared to fed males (**Fig.1C-E**.). To determine if this effect was starvation-specific or a more general neuronal response

to stress, fed males were subjected to proteotoxic (heat shock) or genotoxic (ultraviolet light (UV) exposure) stressors at mid-L4 (**Fig.1B**). 18 hours after stress induction, both heat-shocked and UV-exposed males had increases in DVB neurite outgrowth compared to unstressed animals (**Fig.1C-E**). Thus, three different stressors applied during the mid-L4 stage impacted DVB neuron morphology in a similar manner.

The L4 stage, which is analogous to vertebrate adolescence, is when sexual maturation of the nervous system and other sexual tissues occurs. To test if stress-induced alterations to DVB neuron morphology were specific stressors applied during this adolescent stage, males were stressed either early in the L4 stage, or immediately after entering adulthood (post-L4 molt)(**Fig.1B, Fig.2A, Fig.3A**). Previous work demonstrates that transient fasting of a few hours has similar impact to 18-20 hours of starvation on male muscle and neuron excitability (LeBoeuf, Guo, & Garcia, 2011). While early-L4 heat shock or 4 hour fast resulted in increases in DVB neurite outgrowth (**Fig.1F-G, Fig.3A**), stress immediately following entry into adulthood did not increase DVB neurite outgrowth (**Fig.2**). UV exposure at early L4 resulted in the majority of males arresting before or during the L4 molt, precluding analysis of this stressor at the early L4 timepoint. Interestingly, 18 hour starvation in adult males resulted in a small, but significant, decrease in DVB total neurite length (**Fig.2**). These results suggest that the increase in DVB neurite outgrowth in response to stress is specific to the L4 adolescent stage, and that even a short fasting period of 4 hours during adolescence can alter adult GABAergic neuron morphology.

Two explanations could account for these stress-induced morphologic changes in DVB neurite outgrowth. One possibility is that neurite outgrowth begins earlier in response to stress, such that by the first day of adulthood males have more DVB neurites. Alternatively, DVB neurite outgrowth may start at the same time as in unstressed males, but occur with different dynamics, resulting in adult males with increased neurites. To distinguish between these possibilities, I monitored DVB morphology in unstressed and in early-L4 stressed males at different timepoints from mid L4 into day 1 of adulthood (**Fig.1B**). Strikingly, despite stress being applied during early L4, DVB morphology was not different between non-stressed and stressed males until after the L4 molt and entry into adulthood (**Fig.3A**). At late-L4 and L4 molt, males

had either no neurites or a single short neurite, regardless of stress. Only after L4 molt did differences begin to appear (**Fig.3F-G**). This result supports the second explanation, that adolescent stress does not change the timing of DVB neurite outgrowth, but rather changes the degree of neurite outgrowth occurring in adult males. These results suggest that adolescent stress exposure changes the dynamics of DVB morphologic plasticity in adulthood.

Are stress-induced DVB morphologic changes long-lasting or a temporary and reversible morphologic stress response? DVB morphology was analyzed at day 3 of adulthood following mid-L4 stress (**Fig.3B**). Day 3 of adulthood corresponds to the end of peak male *C. elegans* reproductive capability (Guo, Navetta, Gualberto, & Garcia, 2012). Remarkably, all 3 stressors resulted in increases in at least one parameter of DVB neurite outgrowth more than 60 hours after stress (**Fig.3C,D**). In UV-exposed animals both neurite length and junctions were increased, while in heat shocked males only neurite length was increased, and in starved males only neurite junctions were increased (**Fig.3C,D**). These results demonstrate that although all stressors increase neurites at day 1, different stresses may impact DVB morphology in slightly different ways in the long term (**Fig.3C-D**). Thus, adult DVB neuron morphology is altered by adolescent stress as a consequence of enhanced morphologic plasticity in adulthood, producing long-lasting changes to GABAergic neuron morphology.

Adolescent stressors differentially impact DVB function in male spicule protraction behavior

The functional impact of DVB morphologic plasticity in adulthood was previously characterized on a number of behaviors, including male spicule protraction behavior (Hart & Hobert, 2018). The spicules (**Fig.4A**) protract out of the male tail to penetrate hermaphrodite worms during copulation, and are therefore required for successful sperm transfer (Garcia, Mehta, & Sternberg, 2001). Males exposed to aldicarb, an acetylcholinesterase inhibitor, protract their spicules (**Fig.4A**) due to acetylcholine (ACh) buildup at the neuromuscular synapses between the cholinergic SPC neuron and the spicule protraction muscles (**Fig.4B**)(Garcia et al., 2001). The GABAergic DVB neuron synapses onto the SPC neuron as well as onto the spicule protractor muscles to inhibit

spicule protraction (**Fig.4B**). Therefore, DVB neurite elaboration, which adds synapses specifically onto these targets (Hart & Hobert, 2018), results in increased SPC and spicule protractor inhibition, and a delay in the time to aldicarb-induced spicule protraction. This increased time to spicule protraction serves as a readout for the amount of DVB GABAergic input (Hart & Hobert, 2018).

To test if the outgrowth of DVB neurites induced by adolescent stress impacts the function and plasticity of DVB and the downstream spicule protraction behavior, unstressed and mid-L4-stressed males were exposed to aldicarb at day 1 of adulthood immediately following starvation stress (**Fig.4C**). Starved males had increased time to spicule protraction on aldicarb compared to fed males (**Fig.4C**), suggesting that the elaborated DVB neurites result in functionally enhanced GABAergic tone. In contrast, males exposed to either heat shock or UV had no change in time to spicule protraction in comparison to unstressed males (**Fig.4C**). These results suggest that although all of the stressors result in increased outgrowth of DVB neurites, the functional impact of these neurites is different for each stressor – it is only starvation-induced DVB neurites that have an effect on spicule protraction behavior.

The above data demonstrate that elaborated DVB neurites induced by stress may not have the same impact on circuit connectivity, potentially explaining the disparate behavioral phenotypes. To explore this possibility, I analyzed DVB pre-synaptic puncta in unstressed and mid-L4 stressed males through DVB-specific expression of GFP-tagged RAB-3, a pre-synaptic GTPase. The DVB presynaptic marker in day 1 starved males localized to distinct bright puncta on all DVB neurites, compared with slightly dimmer and more diffuse localization in day 1 non-stressed males, perhaps indicating more mature synaptic structures following starvation (**Fig.4D**). DVB presynaptic puncta in heat shocked and UV exposed males appeared slightly more diffuse with dimmer puncta, and some neurites appearing very dim/diffuse or with no GFP signal (arrowheads, **Fig.4D**). To quantify these potential differences, synaptic puncta were outlined through application of consistent thresholding on confocal z-stack maximum projections using the particle analysis feature in FIJI. A region of interest was drawn around DVB neurites, and particles (puncta) analyzed for various measurements. While there was no difference in the number of puncta between unstressed and any of

the stressed males (data not shown), the average area of puncta in starved males was significantly increased compared to controls, while heat shocked and UV exposed males showed no difference from controls (**Fig.4E**). Additionally, the mean intensity of puncta was also increased in starved males compared to controls, but not males exposed to heat or UV (**Fig.4F**). Thus, starved males appear to have on average larger and brighter DVB presynaptic puncta than controls, a difference not observed in males exposed to heat or UV, which may begin to explain the functional differences observed in behavioral output.

Serotonin signaling is involved in starvation-induced DVB neurite outgrowth and altered spicule protraction behavior

Monoamine signaling is involved in the sensing and signaling of fed and starved states in *C. elegans,* with serotonin serving as a signal for well-fed conditions. It's possible that DVB sensing of starvation stress is through octopamine or serotonin signaling. *C. elegans* with mutations in *tph-1*, the serotonin synthesizing enzyme tryptophan hydroxylase, lack serotonin and recapitulate behaviors of starved animals even when well-fed (Bayer & Hobert, 2018; Chase & Koelle, 2007). To test if serotonin signaling is involved in changes in DVB morphology in response to starvation, I examined DVB morphology in *tph-1* mutant males under fed and starved conditions. DVB in fed *tph-1* mutants had increased neurite outgrowth at day 1 compared to fed controls (**Fig.5A-C**), mimicking starvation-induced changes (**Fig.1C-E**). Furthermore, fed and starved *tph-1* mutants had similar DVB neurite lengths (**Fig.5A,B**), although starved *tph-1* mutants actually had fewer DVB neurite junctions and resembled unstressed wildtype males (**Fig.5C**). Thus, serotonin signaling is likely involved in DVB neuron 'sensation' and response to starvation stress. To test if DVB neurite outgrowth in fed *tph-1* mutants also impacts DVB function, I analyzed fed wildtype and fed *tph-1* mutant males using the aldicarb spicule protraction assay. Males with mutation in *tph-1* had an increase in time to spicule protraction, similar to the increase observed in wildtype males following starvation (**Fig.5D**). Thus, serotonin signaling is involved in DVB neurite outgrowth, and loss of serotonin signaling mimics DVB morphologic and functional changes induced by starvation.

The *C. elegans* neurexin ortholog, *nrx-1,* is required for starvation-induced DVB neurite outgrowth

DVB neurite outgrowth and morphologic plasticity in early adulthood are dependent on the ortholog of the synaptic adhesion molecule neurexin, *nrx-1* (Hart & Hobert, 2018). To determine if stress-induced DVB neurite outgrowth is also dependent on *nrx-1*, I analyzed neurite outgrowth in stressed *nrx-1* mutant males. Two *nrx-1* alleles that strongly reduce gene function but differ in their effects on the two major *nrx-1* isoforms were used: a large deletion that removes the entire short isoform and the transmembrane and intracellular portion of the long isoform (which was recently described to have phenotypes indistinguishable from those of worms with a deletion covering the entire *nrx-1* locus (Kurshan et al., 2018)), or a point mutation resulting in a premature stop codon affecting only the long isoform (**Fig.6A**). As previously observed, loss of *nrx-1* did not impact DVB neurite outgrowth at day 1 under fed conditions (**Fig.6B-D**)(Hart & Hobert, 2018). However, the increase in DVB neurite outgrowth observed in wildtype males following mid-L4 starvation did not occur in males with either mutated allele of *nrx-1*, with DVB neurites in starved *nrx-1* mutant males similar to non-starved wildtype males, and significantly decreased from mid-L4 starved wildtype males (**Fig.6B-D**). Remarkably, DVB neurite outgrowth induced by heat shock or UV exposure was not different in *nrx-1* stressed males with either mutated allele compared to wildtype stressed males (**Fig.7A-F**). These results imply that while DVB neurite outgrowth and morphologic plasticity in response to starvation is dependent on *nrx-1*, heat shock and UV-induced DVB neurite outgrowth is not. Despite all three stressors resulting in increased DVB neurite outgrowth, a role for *nrx-1* is uniquely required for DVB response to starvation. Thus, a defect in a single gene results in loss of neuronal and behavioral stress responses to starvation, but not the UV or heat shock stresses applied here.

To test if *nrx-1* also has an impact on the functional output of DVB neurite outgrowth following adolescent stress, males with *nrx-1* deletion were exposed to mid-L4 stress and the aldicarb spicule protraction assay. Non-stressed *nrx-1* mutants were not different than non-stressed wildtype animals in time to protraction on aldicarb at day

1 (**Fig.8**). Whereas starved wildtype animals were slower to protract spicules on aldicarb than fed wildtype animals, no difference in time to protraction on aldicarb between fed and starved *nrx-1* mutants was observed (**Fig.8**), implicating *nrx-1* in the underlying mechanism responsible for DVB neurite outgrowth and behavioral response to starvation. *nrx-1* males exposed to UV stress had no difference in the time to protraction compared to non-stressed *nrx-1* males (**Fig.8**), similar to UV stress not impacting time to protraction in wildtype animals. Unexpectedly, *nrx-1* males exposed to heat shock had an increase in the time to protraction on aldicarb compared to non-stressed *nrx-1* males (**Fig.6D**), a difference not observed in wildtype males exposed to heat shock (**Fig.4C**). This suggests that even though *nrx-1* plays no role in heat shock-induced DVB morphologic changes, it may play a role in modifying the functional output of DVB or the spicule protraction circuit in response to heat shock, although how and where this occurs will require further investigation. Together, these results show that both the morphologic and functional plasticity of DVB in response to starvation are dependent on *nrx-1*, and demonstrate that different types of stress can have unique behavioral outcomes and depend on different underlying mechanisms.

DISCUSSION

Neurons can respond to stress by altering the morphology of their dendritic trees, altering their connectivity with other neurons within circuits, and thus contributing to alterations in behavioral output (McEwen et al., 2016). Utilizing a recently discovered form of experience-dependent morphologic plasticity in adult male *C. elegans*, I here report that stress induces morphologic remodeling of neurites of a GABAergic neuron and directly impacts behavior. In this study, I find that three stressors during adolescence result in altered morphologic plasticity in the form of increases in axon-like projections of a GABAergic neuron upon entry into adulthood. Remarkably, although each stressor induced increased neurite outgrowth, their effects on a specific behavior (i.e. spicule protraction) was different, which was further reflected in slight differences between stressors on long-term morphologic changes. Interestingly, it is only stressors with a functional impact on behavior that were found to be dependent on *nrx-1* (**Fig.9**); only nutritional stress resulted in both morphologic and functional changes that were

dependent on neurexin. In contrast, genotoxic stress resulted in morphologic changes without any impact on behavior and was not dependent on *nrx-1* (**Fig.9**), while proteotoxic stress also resulted in morphologic changes not dependent on *nrx-1* and without any impact on behavior, but with loss of *nrx-1* uncovering a previously undetectable functional change in the circuit following heat shock. These results suggest that different underlying pathways likely control morphologic and functional changes in response to unique stressors. Together, these findings provide evidence that neuronal morphologic changes in response to stress are dynamic and that different types of stress can have different functional impacts and underlying molecular mechanisms, despite the observation that they all induce changes to neuron morphology. Furthermore, neuronal stress response at the functional level is more complex than a readout of morphologic changes, even in a simple nervous system.

It was recently reported that past life experience, specifically starvation stress, impacts the development of male-specific nervous system wiring in *C. elegans* through monoamine signaling (Bayer & Hobert, 2018). Starvation during development before (L1-L3), but not during adolescence (L4), blocks synaptic pruning events that are required for male-specific circuit wiring and behavior (Bayer & Hobert, 2018; Oren-Suissa, Bayer, & Hobert, 2016). Pre-adolescent starvation stress results in octopamine-regulated depression of serotonin production, producing a 'memory' of starvation in the form of sex-specific connections not being pruned. Interestingly, the results reported here demonstrate that starvation stress during adolescence produces changes in male-specific connectivity through a different mechanism, as a result of altering GABAergic morphologic plasticity. In combination, these results show that early life and adolescent stress both influence the connectivity and behavioral output of sexually dimorphic circuits, the former by impacting the development of sex-specific neuronal connectivity, and the latter by altering the dynamics of an adult form of experience-dependent morphologic plasticity. In both cases, starvation is likely signaled through a reduction in serotonin, conferring connectivity changes through downstream pruning or plasticity mechanisms. The role of serotonin signaling in nervous system regulation of feeding and energy balance is conserved from *C. elegans* to humans (Tecott, 2007), and the serotonin system has been a common therapeutic target for modifying various

neuropsychiatric conditions, including schizophrenia (Terry, Buccafusco, & Wilson, 2008). Indeed there is evidence that therapeutics targeting serotonin may act mechanistically in part through morphologic remodeling and plasticity (Bessa et al., 2009; Umemori, Winkel, Didio, Llach Pou, & Castren, 2018).

Early-life and adolescence are important periods in brain development and maturation marked by reorganization of neurons and circuits in the brain, thereby making these periods sensitive to stress disruption. In adolescence, stress has been shown to impact dendritic morphology of neurons in a number of brain regions, in some cases having a unique impact on morphology and behavior in adolescence compared to the same stress during adulthood (Tsai et al., 2014; Tzanoulinou et al., 2014), with stresses during critical periods in brain development linked to neuropsychiatric disorders. A two-hit model has been proposed where stress during critical brain development windows (early brain development and adolescent maturation) plays a role in the emergence of symptoms. Interestingly, there is evidence that neuron morphology and relevant behavioral phenotypes are impacted differently in animals stressed during both early life and adolescent critical periods of brain development compared to stress during one critical period or in adulthood (Eiland & McEwen, 2012). The results reported here demonstrate that even in the nematode *C. eleganSm,* adolescence and sexual maturation of the nervous system are a period of particular sensitivity to stress.

It has been proposed that to develop models of severe psychiatric disorders, studies should combine genetic variants in susceptibility genes with several stressors during critical periods (Schmitt et al., 2014). Recent work has identified many genetic risk factors for ASDs and schizophrenia that converge on shared pathways, some of which could potentially enhance sensitivity of the nervous system to stress. Neurexin has been associated genetically with ASDs and schizophrenia, but its relationship to neuronal stress response has not been studied. The results reported here indicate that neurexin plays a role in neuronal stress response and promotes morphologic remodeling of GABAergic axons in response to stress. Another adhesion molecule, *NCAM*, has a described role in stress-induced neuronal remodeling, suggesting that multiple cellular adhesion molecules may be important in this process (Gilabert-Juan et al., 2011; McCall et al., 2013). The pathogenic role of *NRXN1* in ASDs and

schizophrenia has been complicated by the presence of deletions/mutations in unaffected parents and siblings, suggesting variable penetrance or involvement of *NRXN1* in these disorders (Lowther et al., 2017; Todarello et al., 2014; Woodbury-Smith et al., 2017). The results reported here in *C. elegans* describe the impact of alteration in a single gene on the morphologic and behavioral consequences of different stress exposures on a singlular neuron, and suggest that some phenotypic heterogeneity may potentially be explained by the requirement for a genetic risk to be uncovered by a specifically timed stress. In terms of neuropsychiatric disease, perhaps multiple genetic risk factors, in combination with different environmental exposures act together to impact the complex human brain, but with varying phenotypic consequences depending on the specific genetic/environmental combination. In fact, a recent study suggests that variation in genetic background in combination with defects in developmental susceptibility genes could explain phenotypic variability (Pizzo et al., 2018), and perhaps stress could also be added to this model. Underlying genetic differences, including defects in susceptibility genes, may only impact some neuronal responses to stress during certain critical periods, which may differ for each stress/genetic risk, adding further complexity and variability to relevant phenotypes.

ACKNOWLEDGEMENTS

I thank Meera Sundaram, David Raizen, Oliver Hobert, Emily Bayer, Laura Pereira, and Theodore G. Drivas for discussions and comments on the included experiments and manuscript; and Meera Sundaram and members of the Sundaram lab for technical support. M.P.H. is supported in part by the Autism Spectrum Program of Excellence at the Perelman School of Medicine. Some strains were provided by the CGC, funded by NIH Office of Research Infrastructure Programs (P40 OD010440).

Author Contributions

M.P.H. conceived, designed, and performed the experiments; analyzed data, and wrote the manuscript.

Author Information

The author declares no conflicts of interest. Correspondence to Michael P. Hart (hartmic@pennmedicine.upenn.edu).

REFERENCES

Autism Spectrum Disorders Working Group of The Psychiatric Genomics, C. (2017). Meta-analysis of GWAS of over 16,000 individuals with autism spectrum disorder highlights a novel locus at 10q24.32 and a significant overlap with schizophrenia. *Mol Autism, 8*, 21. doi:10.1186/s13229-017-0137-9

Bayer, E. A., & Hobert, O. (2018). Past experience shapes sexually dimorphic neuronal wiring through monoaminergic signalling. *Nature, 561*(7721), 117-121. doi:10.1038/s41586-018-0452-0

Bessa, J. M., Ferreira, D., Melo, I., Marques, F., Cerqueira, J. J., Palha, J. A., . . . Sousa, N. (2009). The mood-improving actions of antidepressants do not depend

on neurogenesis but are associated with neuronal remodeling. *Mol Psychiatry, 14*(8), 764-773, 739. doi:10.1038/mp.2008.119

Bishop-Fitzpatrick, L., Mazefsky, C. A., Minshew, N. J., & Eack, S. M. (2015). The relationship between stress and social functioning in adults with autism spectrum disorder and without intellectual disability. *Autism Res, 8*(2), 164-173. doi:10.1002/aur.1433

Cattane, N., Richetto, J., & Cattaneo, A. (2018). Prenatal exposure to environmental insults and enhanced risk of developing Schizophrenia and Autism Spectrum Disorder: focus on biological pathways and epigenetic mechanisms. *Neurosci Biobehav Rev*. doi:10.1016/j.neubiorev.2018.07.001

Chase, D. L., & Koelle, M. R. (2007). Biogenic amine neurotransmitters in C. elegans. *WormBook*, 1-15. doi:10.1895/wormbook.1.132.1

Chaste, P., & Leboyer, M. (2012). Autism risk factors: genes, environment, and gene-environment interactions. *Dialogues Clin Neurosci, 14*(3), 281-292.

Conrad, C. D. (2006). What is the functional significance of chronic stress-induced CA3 dendritic retraction within the hippocampus? *Behav Cogn Neurosci Rev, 5*(1), 41-60. doi:10.1177/1534582306289043

Conrad, C. D., LeDoux, J. E., Magarinos, A. M., & McEwen, B. S. (1999). Repeated restraint stress facilitates fear conditioning independently of causing hippocampal CA3 dendritic atrophy. *Behav Neurosci, 113*(5), 902-913.

Conrad, C. D., Ortiz, J. B., & Judd, J. M. (2017). Chronic stress and hippocampal dendritic complexity: Methodological and functional considerations. *Physiol Behav, 178*, 66-81. doi:10.1016/j.physbeh.2016.11.017

Cook, S. C., & Wellman, C. L. (2004). Chronic stress alters dendritic morphology in rat medial prefrontal cortex. *J Neurobiol, 60*(2), 236-248. doi:10.1002/neu.20025

Czeh, B., Vardya, I., Varga, Z., Febbraro, F., Csabai, D., Martis, L. S., . . . Wiborg, O. (2018). Long-Term Stress Disrupts the Structural and Functional Integrity of GABAergic Neuronal Networks in the Medial Prefrontal Cortex of Rats. *Front Cell Neurosci, 12*, 148. doi:10.3389/fncel.2018.00148

DeBardeleben, H. K., Lopes, L. E., Nessel, M. P., & Raizen, D. M. (2017). Stress-Induced Sleep After Exposure to Ultraviolet Light Is Promoted by p53 in Caenorhabditis elegans. *Genetics, 207*(2), 571-582. doi:10.1534/genetics.117.300070

Eiland, L., & McEwen, B. S. (2012). Early life stress followed by subsequent adult chronic stress potentiates anxiety and blunts hippocampal structural remodeling. *Hippocampus, 22*(1), 82-91. doi:10.1002/hipo.20862

Fuld, S. (2018). Autism Spectrum Disorder: The Impact of Stressful and Traumatic Life Events and Implications for Clinical Practice. *Clin Soc Work J, 46*(3), 210-219. doi:10.1007/s10615-018-0649-6

Garcia, L. R., Mehta, P., & Sternberg, P. W. (2001). Regulation of distinct muscle behaviors controls the C. elegans male's copulatory spicules during mating. *Cell, 107*(6), 777-788.

Gauthier, J., Siddiqui, T. J., Huashan, P., Yokomaku, D., Hamdan, F. F., Champagne, N., . . . Rouleau, G. A. (2011). Truncating mutations in NRXN2 and NRXN1 in autism spectrum disorders and schizophrenia. *Hum Genet, 130*(4), 563-573. doi:10.1007/s00439-011-0975-z

Gilabert-Juan, J., Bueno-Fernandez, C., Castillo-Gomez, E., & Nacher, J. (2017). Reduced interneuronal dendritic arborization in CA1 but not in CA3 region of mice subjected to chronic mild stress. *Brain Behav, 7*(2), e00534. doi:10.1002/brb3.534

Gilabert-Juan, J., Castillo-Gomez, E., Guirado, R., Molto, M. D., & Nacher, J. (2013). Chronic stress alters inhibitory networks in the medial prefrontal cortex of adult mice. *Brain Struct Funct, 218*(6), 1591-1605. doi:10.1007/s00429-012-0479-1

Gilabert-Juan, J., Castillo-Gomez, E., Perez-Rando, M., Molto, M. D., & Nacher, J. (2011). Chronic stress induces changes in the structure of interneurons and in the expression of molecules related to neuronal structural plasticity and inhibitory neurotransmission in the amygdala of adult mice. *Exp Neurol, 232*(1), 33-40. doi:10.1016/j.expneurol.2011.07.009

Guo, X., Navetta, A., Gualberto, D. G., & Garcia, L. R. (2012). Behavioral decay in aging male C. elegans correlates with increased cell excitability. *Neurobiol Aging, 33*(7), 1483 e1485-1423. doi:10.1016/j.neurobiolaging.2011.12.016

Hallmayer, J., Cleveland, S., Torres, A., Phillips, J., Cohen, B., Torigoe, T., . . . Risch, N. (2011). Genetic heritability and shared environmental factors among twin pairs with autism. *Arch Gen Psychiatry, 68*(11), 1095-1102. doi:10.1001/archgenpsychiatry.2011.76

Hart, M. P., & Hobert, O. (2018). Neurexin controls plasticity of a mature, sexually dimorphic neuron. *Nature, 553*(7687), 165-170. doi:10.1038/nature25192

Hertz-Picciotto, I., Schmidt, R. J., & Krakowiak, P. (2018). Understanding environmental contributions to autism: Causal concepts and the state of science. *Autism Res, 11*(4), 554-586. doi:10.1002/aur.1938

Jiang, Z., Cowell, R. M., & Nakazawa, K. (2013). Convergence of genetic and environmental factors on parvalbumin-positive interneurons in schizophrenia. *Front Behav Neurosci, 7*, 116. doi:10.3389/fnbeh.2013.00116

Kagias, K., Nehammer, C., & Pocock, R. (2012). Neuronal responses to physiological stress. *Front Genet, 3*, 222. doi:10.3389/fgene.2012.00222

Kirov, G., Rujescu, D., Ingason, A., Collier, D. A., O'Donovan, M. C., & Owen, M. J. (2009). Neurexin 1 (NRXN1) deletions in schizophrenia. *Schizophr Bull, 35*(5), 851-854. doi:10.1093/schbul/sbp079

Kurshan, P. T., Merrill, S. A., Dong, Y., Ding, C., Hammarlund, M., Bai, J., . . . Shen, K. (2018). gamma-Neurexin and Frizzled Mediate Parallel Synapse Assembly Pathways Antagonized by Receptor Endocytosis. *Neuron, 100*(1), 150-166 e154. doi:10.1016/j.neuron.2018.09.007

LeBoeuf, B., Guo, X., & Garcia, L. R. (2011). The effects of transient starvation persist through direct interactions between CaMKII and ether-a-go-go K+ channels in C. elegans males. *Neuroscience, 175*, 1-17. doi:10.1016/j.neuroscience.2010.12.002

Locke, C., Berry, K., Kautu, B., Lee, K., Caldwell, K., & Caldwell, G. (2008). Paradigms for pharmacological characterization of C. elegans synaptic transmission mutants. *J Vis Exp*(18). doi:10.3791/837

Longair, M. H., Baker, D. A., & Armstrong, J. D. (2011). Simple Neurite Tracer: open source software for reconstruction, visualization and analysis of neuronal processes. *Bioinformatics, 27*(17), 2453-2454. doi:10.1093/bioinformatics/btr390

Lowther, C., Speevak, M., Armour, C. M., Goh, E. S., Graham, G. E., Li, C., . . . Bassett, A. S. (2017). Molecular characterization of NRXN1 deletions from 19,263 clinical microarray cases identifies exons important for neurodevelopmental disease expression. *Genet Med, 19*(1), 53-61. doi:10.1038/gim.2016.54

McCall, T., Weil, Z. M., Nacher, J., Bloss, E. B., El Maarouf, A., Rutishauser, U., & McEwen, B. S. (2013). Depletion of polysialic acid from neural cell adhesion molecule (PSA-NCAM) increases CA3 dendritic arborization and increases vulnerability to excitotoxicity. *Exp Neurol, 241*, 5-12. doi:10.1016/j.expneurol.2012.11.028

McEwen, B. S., Nasca, C., & Gray, J. D. (2016). Stress Effects on Neuronal Structure: Hippocampus, Amygdala, and Prefrontal Cortex. *Neuropsychopharmacology, 41*(1), 3-23. doi:10.1038/npp.2015.171

McKlveen, J. M., Morano, R. L., Fitzgerald, M., Zoubovsky, S., Cassella, S. N., Scheimann, J. R., . . . Herman, J. P. (2016). Chronic Stress Increases Prefrontal Inhibition: A Mechanism for Stress-Induced Prefrontal Dysfunction. *Biol Psychiatry, 80*(10), 754-764. doi:10.1016/j.biopsych.2016.03.2101

Oren-Suissa, M., Bayer, E. A., & Hobert, O. (2016). Sex-specific pruning of neuronal synapses in Caenorhabditis elegans. *Nature, 533*(7602), 206-211. doi:10.1038/nature17977

Pizzo, L., Jensen, M., Polyak, A., Rosenfeld, J. A., Mannik, K., Krishnan, A., . . . Girirajan, S. (2018). Rare variants in the genetic background modulate cognitive and developmental phenotypes in individuals carrying disease-associated variants. *Genet Med*. doi:10.1038/s41436-018-0266-3

Reichelt, A. C., Rodgers, R. J., & Clapcote, S. J. (2012). The role of neurexins in schizophrenia and autistic spectrum disorder. *Neuropharmacology, 62*(3), 1519-1526. doi:10.1016/j.neuropharm.2011.01.024

Sandin, S., Lichtenstein, P., Kuja-Halkola, R., Larsson, H., Hultman, C. M., & Reichenberg, A. (2014). The familial risk of autism. *JAMA, 311*(17), 1770-1777. doi:10.1001/jama.2014.4144

Schmitt, A., Hasan, A., Gruber, O., & Falkai, P. (2011). Schizophrenia as a disorder of disconnectivity. *Eur Arch Psychiatry Clin Neurosci, 261 Suppl 2*, S150-154. doi:10.1007/s00406-011-0242-2

Schmitt, A., Malchow, B., Hasan, A., & Falkai, P. (2014). The impact of environmental factors in severe psychiatric disorders. *Front Neurosci, 8*, 19. doi:10.3389/fnins.2014.00019

Snoek, L. B., Sterken, M. G., Volkers, R. J., Klatter, M., Bosman, K. J., Bevers, R. P., . . . Kammenga, J. E. (2014). A rapid and massive gene expression shift marking adolescent transition in C. elegans. *Sci Rep, 4*, 3912. doi:10.1038/srep03912

Sudhof, T. C. (2017). Synaptic Neurexin Complexes: A Molecular Code for the Logic of Neural Circuits. *Cell, 171*(4), 745-769. doi:10.1016/j.cell.2017.10.024

Tecott, L. H. (2007). Serotonin and the orchestration of energy balance. *Cell Metab, 6*(5), 352-361. doi:10.1016/j.cmet.2007.09.012

Terry, A. V., Jr., Buccafusco, J. J., & Wilson, C. (2008). Cognitive dysfunction in neuropsychiatric disorders: selected serotonin receptor subtypes as therapeutic targets. *Behav Brain Res, 195*(1), 30-38. doi:10.1016/j.bbr.2007.12.006

Tick, B., Bolton, P., Happe, F., Rutter, M., & Rijsdijk, F. (2016). Heritability of autism spectrum disorders: a meta-analysis of twin studies. *J Child Psychol Psychiatry, 57*(5), 585-595. doi:10.1111/jcpp.12499

Todarello, G., Feng, N., Kolachana, B. S., Li, C., Vakkalanka, R., Bertolino, A., . . . Straub, R. E. (2014). Incomplete penetrance of NRXN1 deletions in families with schizophrenia. *Schizophr Res, 155*(1-3), 1-7. doi:10.1016/j.schres.2014.02.023

Tsai, S. F., Huang, T. Y., Chang, C. Y., Hsu, Y. C., Chen, S. J., Yu, L., . . . Jen, C. J. (2014). Social instability stress differentially affects amygdalar neuron adaptations and memory performance in adolescent and adult rats. *Front Behav Neurosci, 8*, 27. doi:10.3389/fnbeh.2014.00027

Tzanoulinou, S., Garcia-Mompo, C., Castillo-Gomez, E., Veenit, V., Nacher, J., & Sandi, C. (2014). Long-term behavioral programming induced by peripuberty stress in rats is accompanied by GABAergic-related alterations in the Amygdala. *PLoS One, 9*(4), e94666. doi:10.1371/journal.pone.0094666

Umemori, J., Winkel, F., Didio, G., Llach Pou, M., & Castren, E. (2018). iPlasticity: Induced juvenile-like plasticity in the adult brain as a mechanism of antidepressants. *Psychiatry Clin Neurosci, 72*(9), 633-653. doi:10.1111/pcn.12683

Vyas, A., Mitra, R., Shankaranarayana Rao, B. S., & Chattarji, S. (2002). Chronic stress induces contrasting patterns of dendritic remodeling in hippocampal and amygdaloid neurons. *J Neurosci, 22*(15), 6810-6818. doi:20026655

Waltereit, R., Banaschewski, T., Meyer-Lindenberg, A., & Poustka, L. (2014). Interaction of neurodevelopmental pathways and synaptic plasticity in mental retardation, autism spectrum disorder and schizophrenia: implications for psychiatry. *World J Biol Psychiatry, 15*(7), 507-516. doi:10.3109/15622975.2013.838641

Woodbury-Smith, M., Nicolson, R., Zarrei, M., Yuen, R. K. C., Walker, S., Howe, J., . . . Scherer, S. W. (2017). Variable phenotype expression in a family segregating microdeletions of the NRXN1 and MBD5 autism spectrum disorder susceptibility genes. *NPJ Genom Med, 2*. doi:10.1038/s41525-017-0020-9

Yizhar, O., Fenno, L. E., Prigge, M., Schneider, F., Davidson, T. J., O'Shea, D. J., . . . Deisseroth, K. (2011). Neocortical excitation/inhibition balance in information processing and social dysfunction. *Nature, 477*(7363), 171-178. doi:10.1038/nature10360

FIGURE LEGENDS

Figure 1. Multiple stressors during adolescence induce neurite outgrowth of DVB neuron in adult male *C. elegans*. A) Illustration of male *C. elegans* with DVB neuron and neurites depicted. **B)** Timeline of post-embryonic development of male *C. elegans* with inset of L4 to adult period. Boxes below timeline indicate timing of different stressors labeled for each panel; grey – control/fed, magenta – starvation/fasting, teal – heat shock, green – UV exposure. Asterisk indicates time of confocal imaging and DVB neurite quantification. **C)** Confocal z-stack maximum projections of DVB neuron in control and mid-L4 stressed males at day 1 of adulthood (arrowheads indicate DVB neurites, white asterisk indicates soma of PVT neuron, scale bar = 10µm). Quantification of (**D**) total neurite length and (**E**) neurite junctions for DVB in control and mid-L4 stressed males at day 1 (Each dot represents one worm; colored bar, median; boxes, quartiles. Comparison using one-way ANOVA and post-hoc Tukey HSD, *P* values shown above plots with bold showing significance ($P<0.05$). True for all

subsequent Figures). Quantification of (**F**) total neurite length and (**G**) neurite junctions for DVB in control and early-L4 stressed males at day 1, corresponding confocal maximum projections included as day 1 panel of Fig.3A.

Figure 2. Stressors in early adulthood do not increase DVB neurite outgrowth. A) Diagram of L4 to adult period with boxes depicting stressors applied following entry into adulthood after the L4 molt. Quantification of (**B**) total neurite length and (**C**) neurite junctions for DVB in control and post-L4 molt stressed males.

Figure 3. Adolescent stress alters DVB adult neurite outgrowth dynamics and results in sustained changes to DVB morphology. A) Confocal z-stack maximum projections of DVB neuron in control and early-L4 stressed males at different times throughout the L4 stage into early adulthood (10 males observed for each timepoint and condition)(scale bar = 10µm). **B)** Diagram of L4 to adult period, including inset indicating day 3 of adulthood. Boxes below timeline indicate timing of stressors, asterisk indicates time of confocal imaging and quantification. Quantification of (**C**) total neurite length and (**D**) neurite junctions for DVB in control and mid-L4 stressed males at day 3.

Figure 4. Adolescent stress differentially impacts adult spicule protraction behavior and DVB presynaptic morphology A) Cartoon of *C. elegans* male tail with DVB and spicules depicted in retracted and protracted positions. **B)** Logic diagram of the male *C. elegans* spicule protraction circuit involving DVB GABAergic and SPC cholinergic signaling, showing location of action of the acetylcholinesterase inhibitor aldicarb. **C)** Time to protraction of spicules in control and mid-L4 stressed males on aldicarb plates at day 1 of adulthood. **D)** Confocal z-stack maximum projections of DVB neuron and DVB presynaptic puncta (*lim-6^{int4}::rab-3::gfp*) in control and mid-L4 stressed males at day 1 of adulthood (arrowheads indicate DVB neurites with little/no gfp or diffuse gfp, scale bar = 10µm). Identically thresholded z-stack maximum projections of the *rab-3::gfp* channel created particle outlines of synaptic puncta on DVB neurites for analysis of intensity and other measures. Quantification of *lim-6^{int4}::rab-3::gfp* (**E**)

average particle area and (**F**) average mean intensity in control and mid-L4 stressed males at day 1.

Figure 5. Loss of serotonin signaling induces adult DVB neurite outgrowth in non-stressed males. A) Confocal z-stack maximum projections of DVB neuron in fed control, fed *tph-1(n4662)*, and mid-L4 starved *tph-1(n4662)* males at day 1 of adulthood (scale bar = 10μm). Quantification of (**B**) total neurite length and (**C**) neurite junctions for DVB in fed control, fed *tph-1(n4662)*, and mid-L4 starved *tph-1(n4662)* males at day 1. **D)** Time to protraction of spicules in fed control and fed *tph-1(n4662)* males on aldicarb plates at day 1 of adulthood.

Figure 6. Neurexin is required for DVB neurite outgrowth following starvation stress. A) Genomic locus of *nrx-1* shown 5' to 3' with long and short isoforms included, red bar indicates region deleted in *nrx-1(wy778)* and red asterisk indicates point mutation of early stop in *nrx-1(gk246237)* referred to in Figures as *nrx-1(gk)*. **B)** Confocal z-stack maximum projections of DVB neuron in fed control and mid-L4 starved control, *nrx-1(wy778)*, and *nrx-1(gk246237)* males at day 1 of adulthood (scale bar = 10μm). Quantification of (**C**) total neurite length and (**D**) neurite junctions for DVB in fed and mid-L4 starved control, *nrx-1(wy778)*, and *nrx-1(gk246237))* males at day 1.

Figure 7. Neurexin is not required for DVB neurite outgrowth following proteotoxic or genotoxic stress. A) Confocal z-stack maximum projections of DVB neuron in control, and mid-L4 heat shocked control, *nrx-1(wy778)*, and *nrx-1(gk246237)* males at day 1 of adulthood (scale bar = 10μm). Quantification of (**B**) total neurite length and (**C**) neurite junctions for DVB in control, and mid-L4 heat shocked control, *nrx-1(wy778)*, and *nrx-1(gk246237)* males at day 1. **D)** Confocal z-stack maximum projections of DVB neuron in control, and mid-L4 UV exposed control, *nrx-1(wy778)*, and *nrx-1(gk246237)* males at day 1 of adulthood (scale bar = 10μm). Quantification of (**E**) total neurite length and (**F**) neurite junctions for DVB in control, and mid-L4 UV exposed control, *nrx-1(wy778)*, and *nrx-1(gk246237)* males at day 1.

Figure 8. *nrx-1* is required for starvation-induced increase in time to spicule protraction. Time to protraction of spicules in fed control, starved control (repeated data from Fig.3C, for comparison), and mid-L4 control and stressed *nrx-1(wy778)* males on aldicarb plates at day 1 of adulthood.

Figure 9. Model of adolescent stress impacting adult DVB neuron morphology, dependence on neurexin, and behavior. DVB in non-stressed males at day 1 has few neurites and immature synapses (dim and small) that will grow out in response to experience during adulthood. Adolescent starvation increases DVB neurite outgrowth at day 1 of adulthood, downstream of reduced serotonin signaling, resulting in more developed synapses (more area and brighter) that are dependent on *nrx-1*, and result in longer time to spicule protraction. Males exposed to UV or heat shock have increased DVB neurite outgrowth at day 1 that is not dependent on *nrx-1*, and with no change in spicule protraction behavior, likely due to synapses remaining less developed (less area and dimmer than starvation), similar to DVB synapses in unstressed day 1 males.

MATERIALS AND METHODS

C. elegans strains

Wild-type strains were *C. elegans* variety Bristol, strain N2. Worms were grown at 23 °C on nematode growth media (NGM) plates seeded with bacteria (*E.coli* OP50) as a food source. All males contained either *him-8(e1489) IV* or *him-5(e1490) V* as indicated by strain.

Mutant alleles used in this study include:
him-8(e1489) IV, him-5(e1490) V, tph-1(n4662), unc-119(ed3) III; nrx-1(wy778[unc-119(+)]) V, nrx-1(gk246237).

All transgenic strains used in this study are listed in **Table 1** ordered by Figures.

Stress induction

Male worms were picked at early-L4, mid-L4, or following L4 molt (adulthood) as

indicated in Figures onto plates described below with 10 other males. Non-stressed males were placed onto NGM plates with OP50 as a food source at 23°C. Starved and fasted males were placed onto NGM plates lacking peptone and any food source at times indicated and for duration indicated (18 hours or 4 hours), then analyzed or returned to NGM plates with OP50 as a food source. Heat shock was performed by placing males onto NGM plates with OP50 as a food source, setting the plate in a 37°C incubator for 30 minutes, then returning plate to 23°C. For ultraviolet (UV) exposure males were placed on NGM plates with a thin layer of OP50 as a food source to minimize blocking UV rays, which was set in a Spectrolinker XL-1500 (Spectroline) uncovered, and irradiated with 254 nm light using the energy input function which varies the exposure time(DeBardeleben, Lopes, Nessel, & Raizen, 2017), here set to 200 X100 μJ/cm^2. In all non-stress and stress conditions, males were subjected to image analysis or behavioral assays at times indicated in Figures.

Microscopy

Worms were anesthetized using 5 μl of 100 mM of sodium azide (NaN_3) on a pad of 5% agarose on glass slides, and covered with a glass coverslip. Worms were analyzed by fluorescence microscopy, using an upright stand Leica TCS SP8 laser-scanning microscope operated by LAS X software. Confocal laser and photomultiplier tube settings were set at identical levels for image acquisition of all experimental conditions. Confocal z-stacks were reconstructed as maximum intensity projections in FIJI. Figures were prepared using Adobe Photoshop CS6 and Adobe Illustrator CS6.

Neurite tracing

Neurite tracing was performed as previously described(Hart & Hobert, 2018). Briefly, confocal z-stacks were opened in FIJI, and analyzed using the Simple Neurite Tracer plugin(Longair, Baker, & Armstrong, 2011). The primary neurite of DVB was traced from the center of the cell soma to where the axon projects ventrally and turns anteriorly into the ventral nerve cord. Neurite branches were added by tracing off the primary neurite, including all neurites emanating posterior of the last branch point. The simple neurite tracer plugin was used to analyze the skeletons for neurite length, which were summed

to calculate total neurite length, and the number of neurite junctions (a proxy for the number of neurite branches).

Aldicarb spicule protraction assay

Aldicarb solution was added on the top of NGM agar plates and allowed to dry for 1 hour with plate lid on. For a concentration of 0.8 mM aldicarb, 80 ul of a 100 mM in 70% ethanol stock solution was added onto 10 ml NGM plates and spread evenly on surface(Locke et al., 2008). 10 male worms were placed onto the aldicarb plates and observed for spicule protraction longer than 3s, when the time was recorded for each worm. Aldicarb assay was performed on 2 technical replicates and at least 3 independent replicates. Investigator was blinded to experimental conditions before aldicarb assay was performed.

Particle analysis of *rab-3::gfp* synaptic puncta

Confocal z-stacks were opened and turned into maximum projections in FIJI. A region of interest was drawn around all of the neurites of DVB, defined the same way as for neurite tracing. Particles, representing synaptic puncta, were defined by manual thresholding of projections (top slider 20, bottom slider 255) and subsequent particle analysis to outline particles. Without applying threshold, these regions were then analyzed using Analyze Particle tool. Particle number, particle area, and mean particle intensity were determined for each particle and used to determine total particle number, mean particle area, and mean particle intensity for each worm.

Statistics and reproducibility

One-way ANOVA with post-hoc Tukey HSD tests were performed using *RStudio*, p-values shown on each graph. Beeswarm and boxplot graphs were created in *RStudio.*

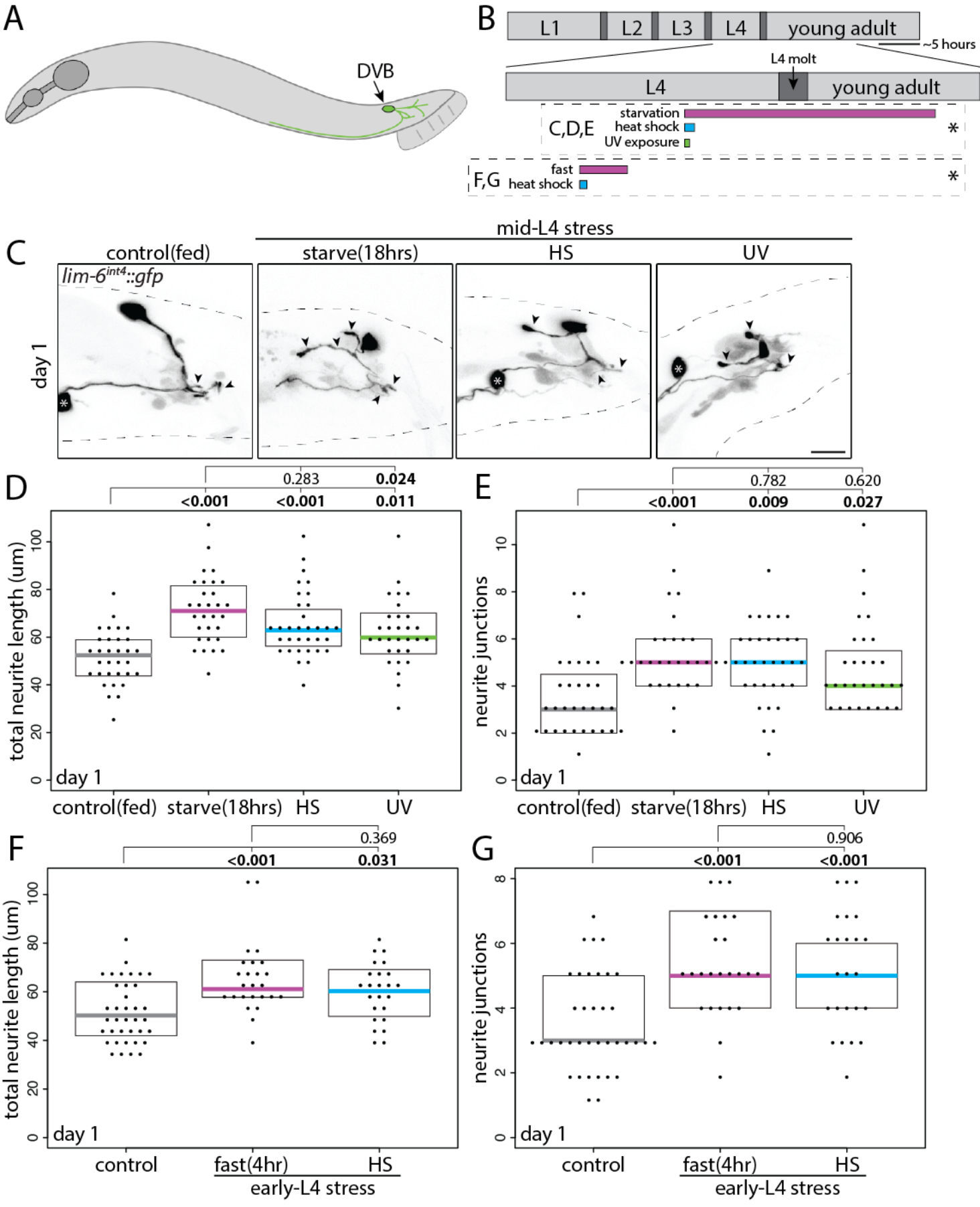
A
DVB
B
L1
L2
L3
L4
young adult
~5 hours
L4 molt
L4
young adult
C,D,E
starvation
heat shock
UV exposure
*
F,G
fast
heat shock
*
C
mid-L4 stress
control(fed)
starve(18hrs)
HS
UV
lim-6int4::gfp
day 1
D
0.283
0.024
<0.001
<0.001
0.011
total neurite length (um)
day 1
control(fed)
starve(18hrs)
HS
UV
E
0.782
0.620
<0.001
0.009
0.027
neurite junctions
day 1
control(fed)
starve(18hrs)
HS
UV
F
0.369
<0.001
0.031
total neurite length (um)
day 1
control
fast(4hr)
HS
early-L4 stress
G
0.906
<0.001
<0.001
neurite junctions
day 1
control
fast(4hr)
HS
early-L4 stress

FIGURE 1

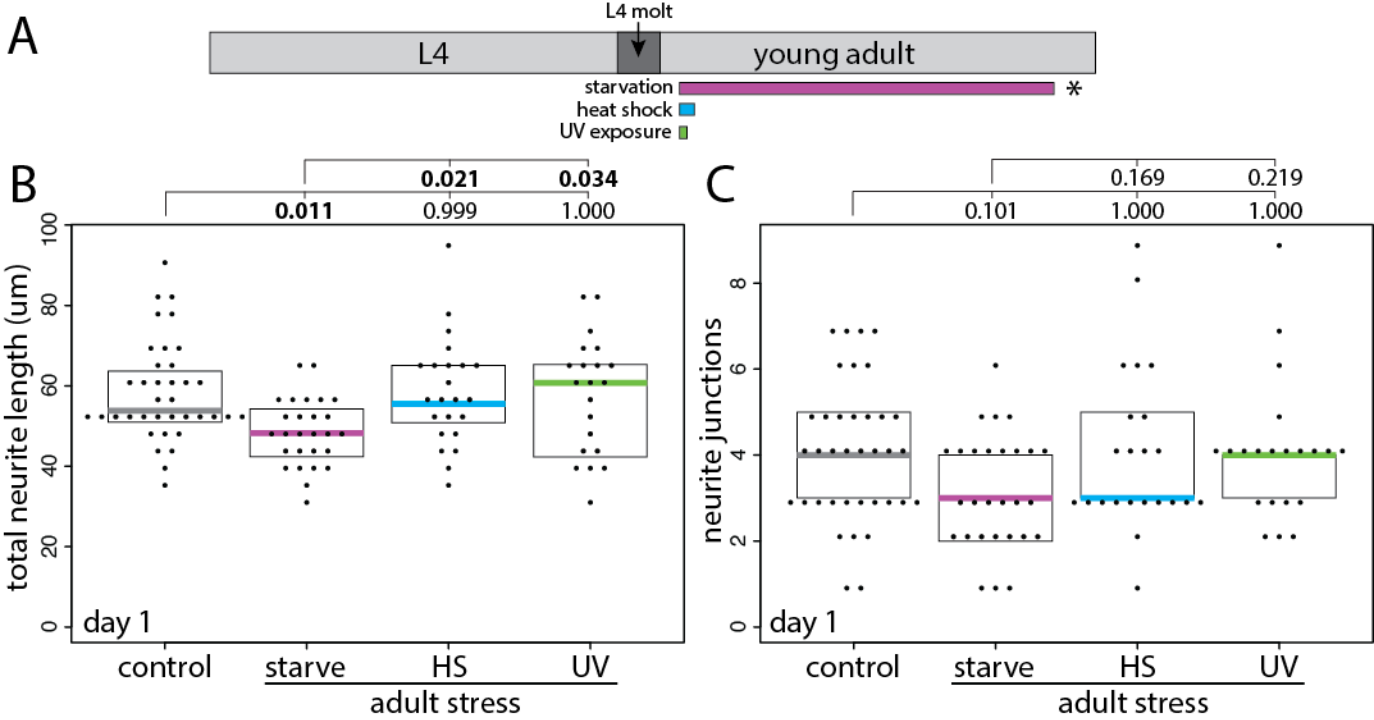
A
L4 molt
L4
young adult
starvation
heat shock
UV exposure
*
B
0.021
0.034
0.011
0.999
1.000
total neurite length (um)
0
20
40
60
80
100
day 1
control
starve
HS
UV
adult stress
C
0.169
0.219
0.101
1.000
1.000
neurite junctions
0
2
4
6
8
day 1
control
starve
HS
UV
adult stress

Figure 2

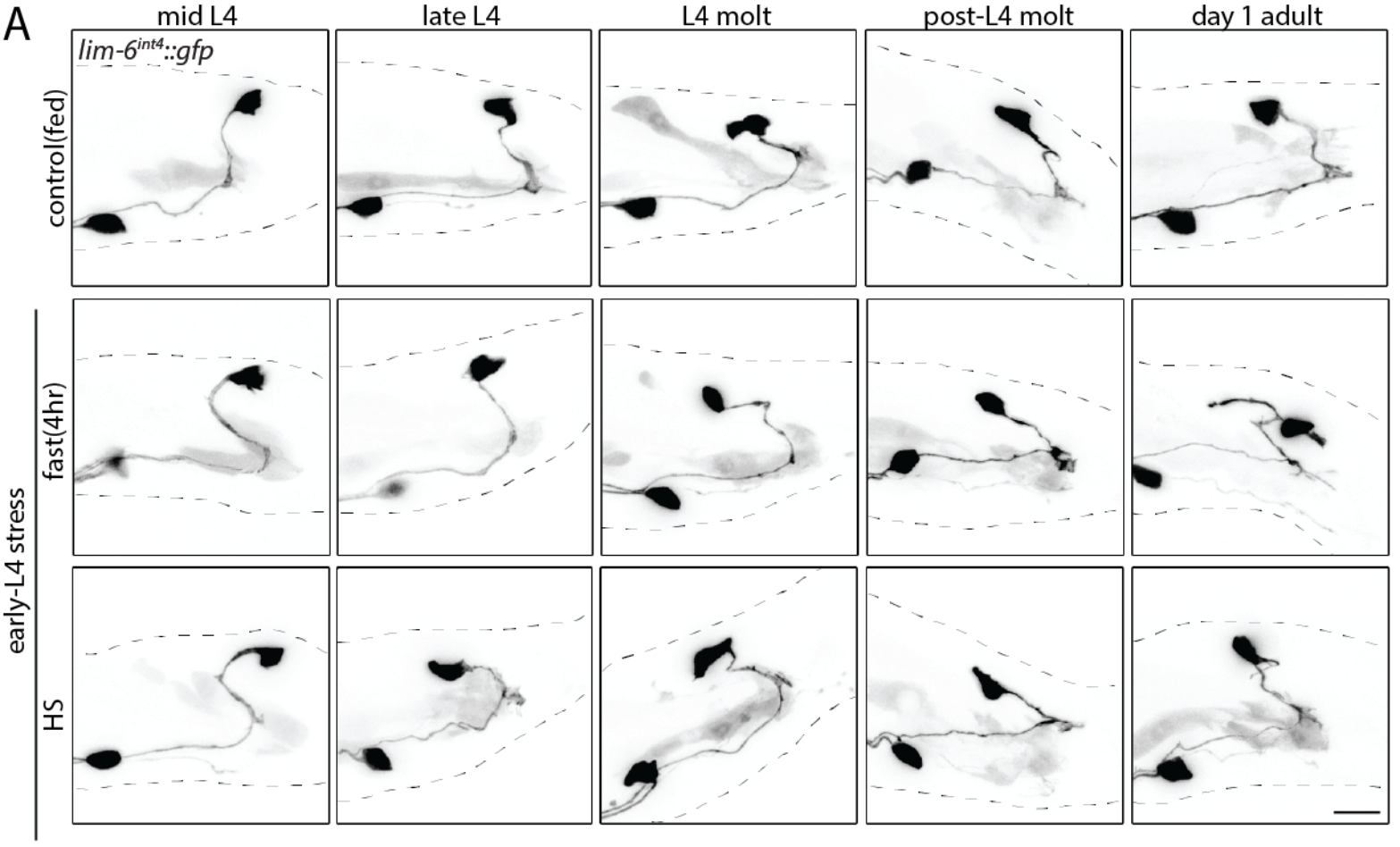
A
mid L4
late L4
L4 molt
post-L4 molt
day 1 adult
lim-6int4::gfp
control(fed)
early-L4 stress
fast(4hr)
HS

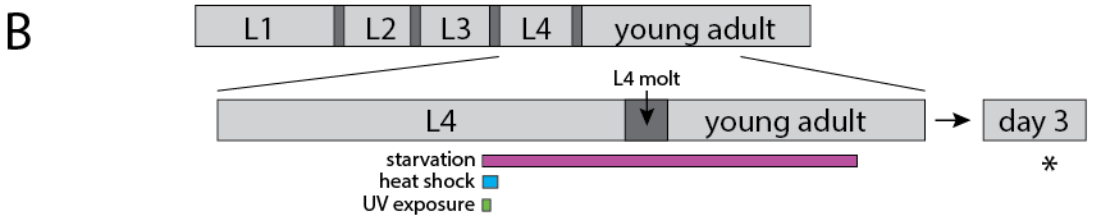
B
L1
L2
L3
L4
young adult
L4 molt
L4
young adult
day 3
starvation
heat shock
UV exposure
*

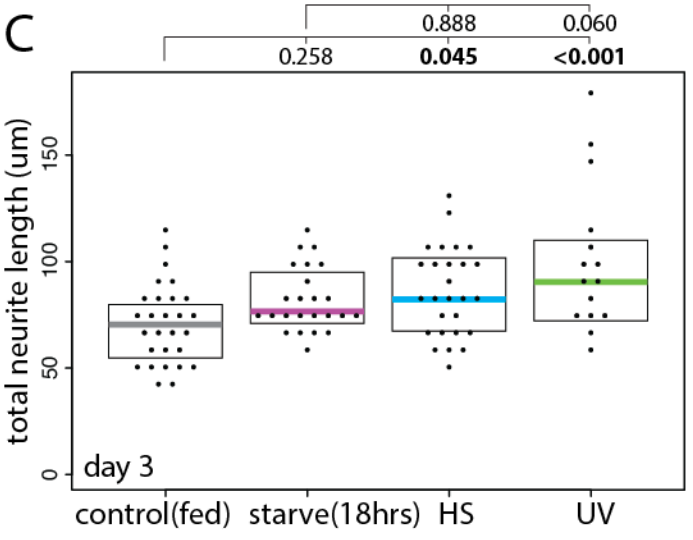
C
0.258
0.888
0.045
0.060
<0.001
total neurite length (um)
0
50
100
150
day 3
control(fed)
starve(18hrs)
HS
UV

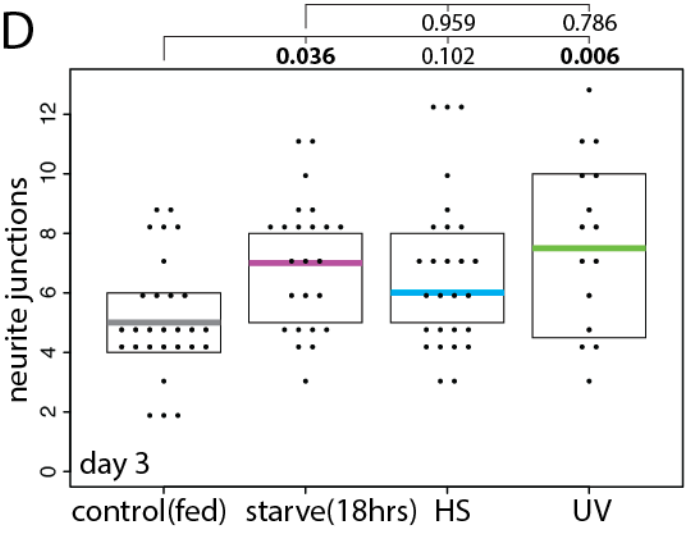
D
0.036
0.959
0.102
0.786
0.006
neurite junctions
0
2
4
6
8
10
12
day 3
control(fed)
starve(18hrs)
HS
UV

FIGURE 3

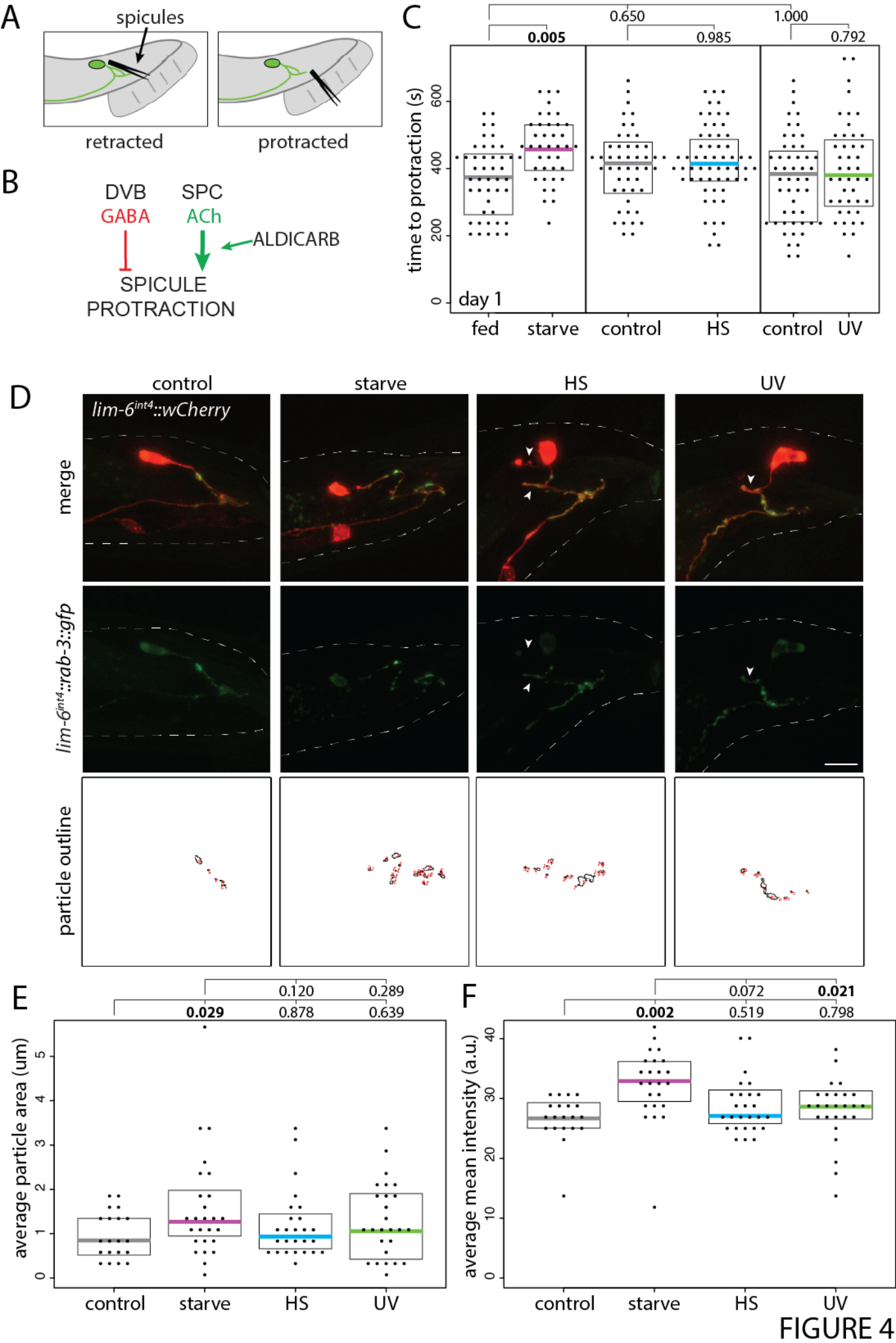
A
spicules
retracted
protracted
B
DVB
GABA
SPC
ACh
ALDICARB
SPICULE
PROTRACTION
C
0.650
1.000
0.005
0.985
0.792
time to protraction (s)
day 1
fed
starve
control
HS
control
UV
D
control
starve
HS
UV
lim-6int4::wCherry
merge
lim-6int4::rab-3::gfp
particle outline
E
0.120
0.289
0.029
0.878
0.639
average particle area (um)
control
starve
HS
UV
F
0.072
0.021
0.002
0.519
0.798
average mean intensity (a.u.)
control
starve
HS
UV

FIGURE 4

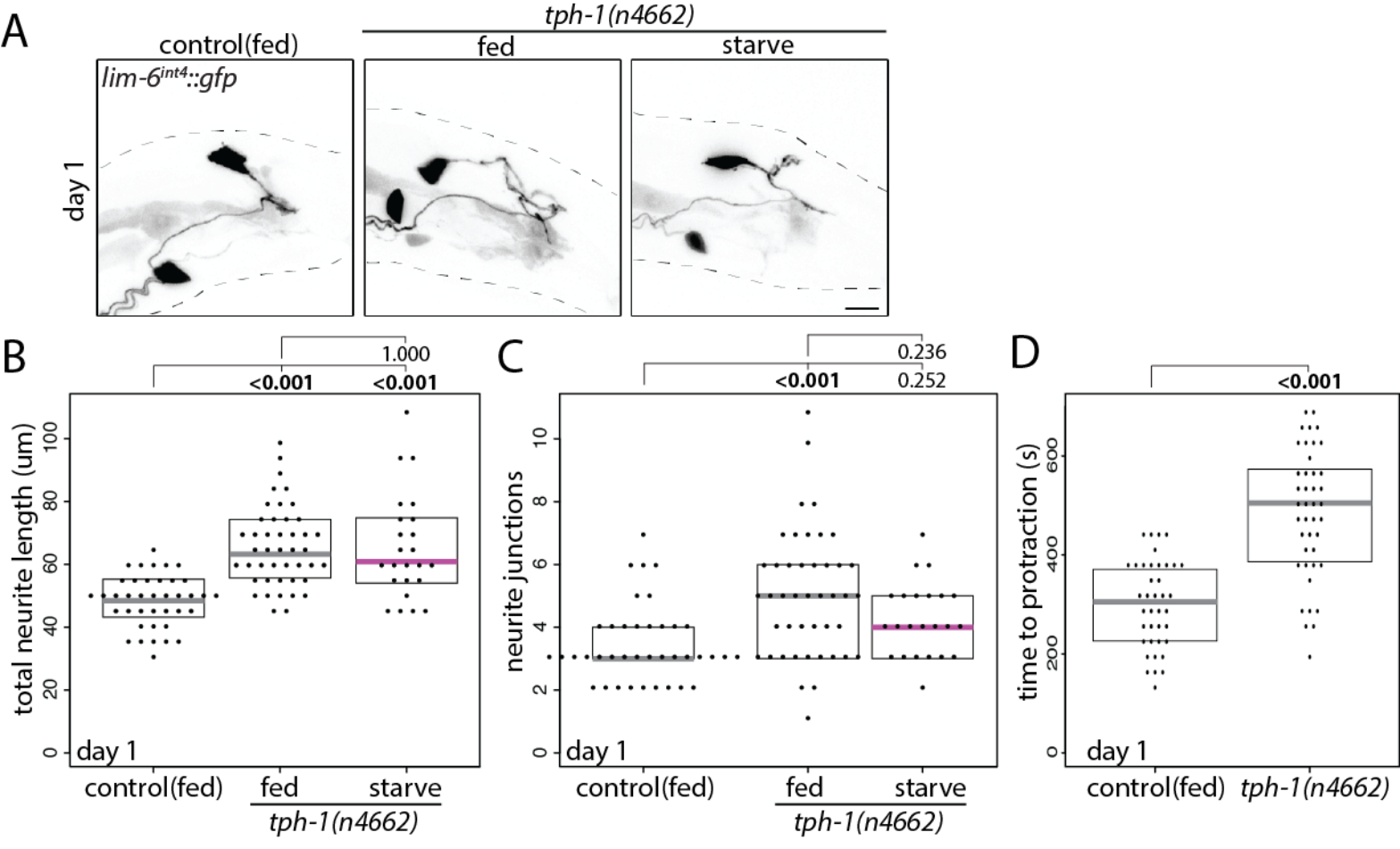
A
tph-1(n4662)
control(fed)
fed
starve
lim-6int4::gfp
day 1
B
1.000
<0.001
<0.001
total neurite length (um)
0
20
40
60
80
100
day 1
control(fed)
fed
starve
tph-1(n4662)
C
0.236
<0.001
0.252
neurite junctions
0
2
4
6
8
10
day 1
control(fed)
fed
starve
tph-1(n4662)
D
<0.001
time to protraction (s)
0
200
400
600
day 1
control(fed)
tph-1(n4662)

FIGURE 5

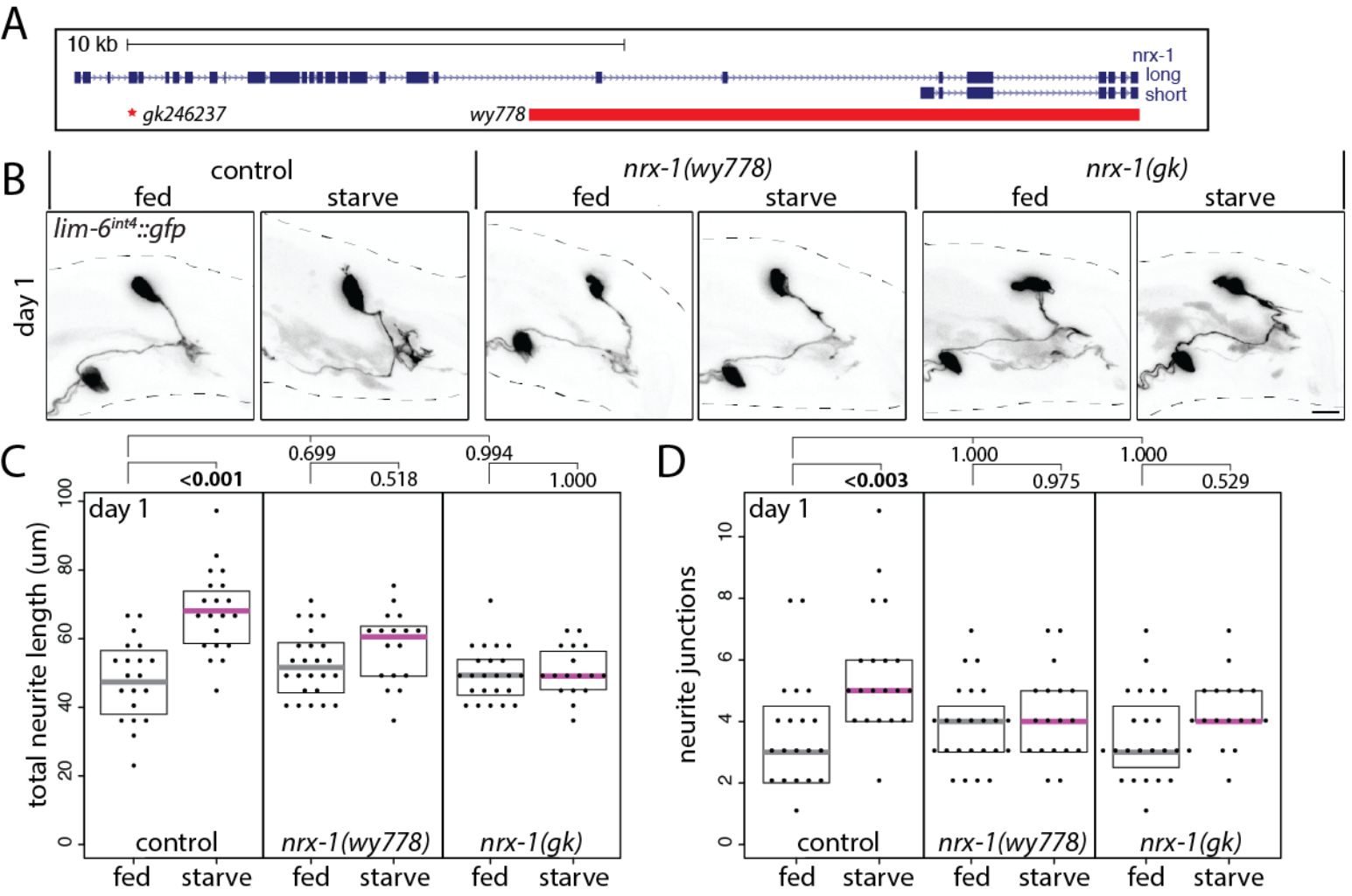
A
10 kb
nrx-1
long
short
gk246237
wy778
B
control
nrx-1(wy778)
nrx-1(gk)
fed
starve
lim-6int4::gfp
day 1
C
0.699
0.994
<0.001
0.518
1.000
day 1
total neurite length (um)
control
nrx-1(wy778)
nrx-1(gk)
D
1.000
1.000
<0.003
0.975
0.529
neurite junctions

FIGURE 6

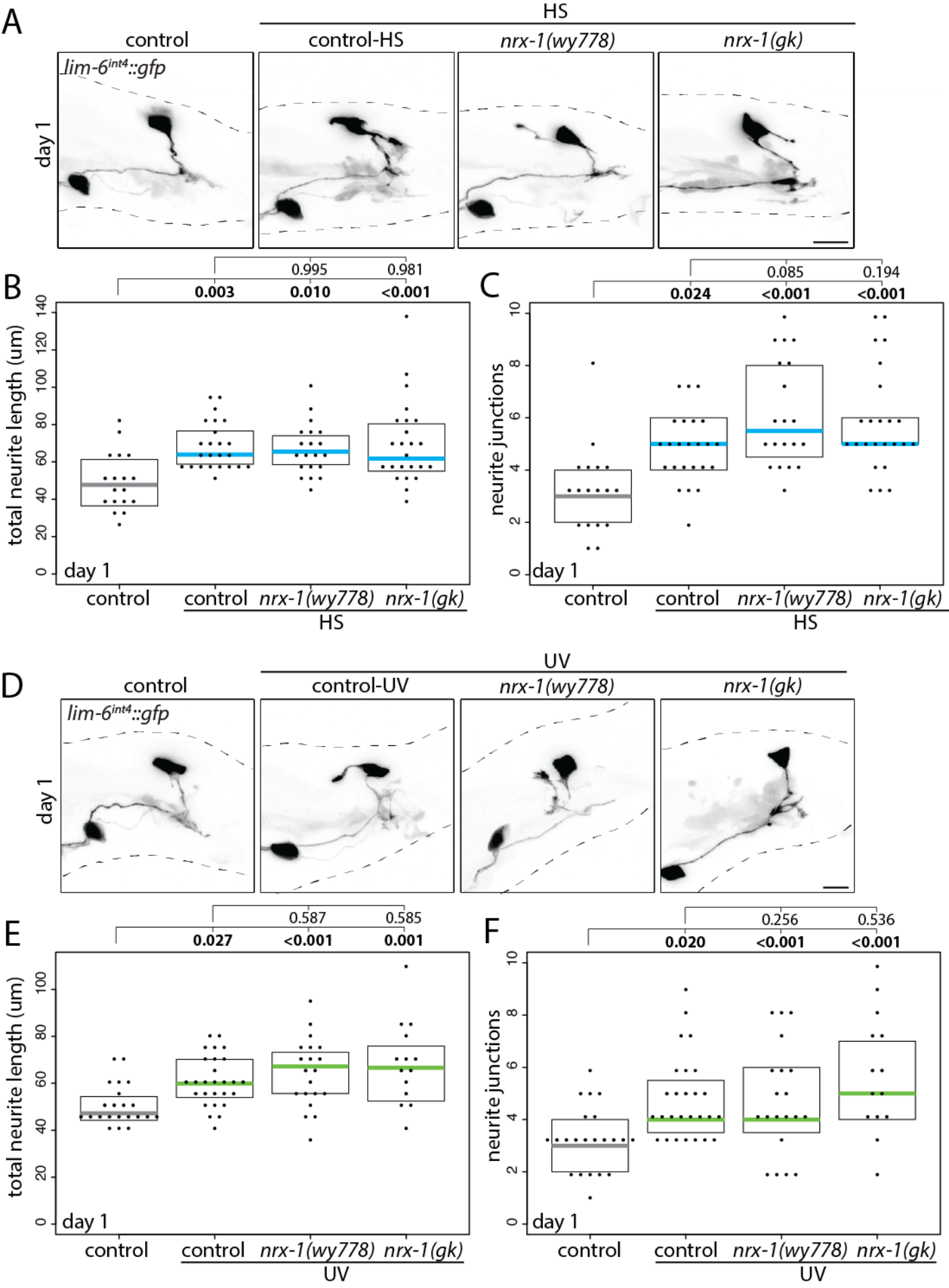
A
HS
control
control-HS
nrx-1(wy778)
nrx-1(gk)
lim-6int4::gfp
day 1
B
0.995
0.981
0.003
0.010
<0.001
total neurite length (um)
day 1
control
control
nrx-1(wy778)
nrx-1(gk)
HS
C
0.085
0.194
0.024
<0.001
<0.001
neurite junctions
day 1
control
control
nrx-1(wy778)
nrx-1(gk)
HS
D
UV
control
control-UV
nrx-1(wy778)
nrx-1(gk)
lim-6int4::gfp
day 1
E
0.587
0.585
0.027
<0.001
0.001
total neurite length (um)
day 1
control
control
nrx-1(wy778)
nrx-1(gk)
UV
F
0.256
0.536
0.020
<0.001
<0.001
neurite junctions
day 1
control
control
nrx-1(wy778)
nrx-1(gk)
UV

FIGURE 7

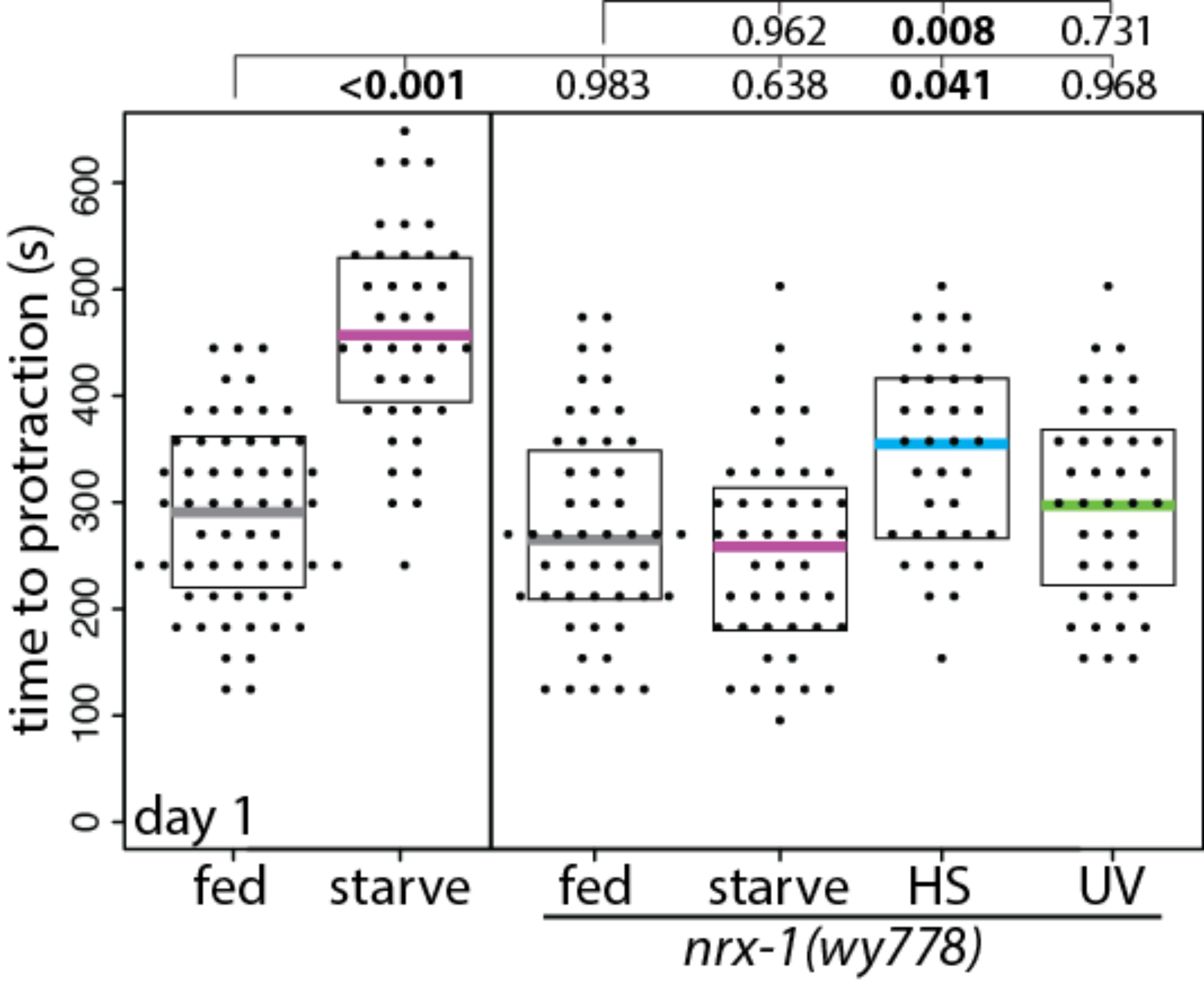
0.962
0.008
0.731
<0.001
0.983
0.638
0.041
0.968
time to protraction (s)
0
100
200
300
400
500
600
day 1
fed
starve
fed
starve
HS
UV
nrx-1(wy778)

FIGURE 8

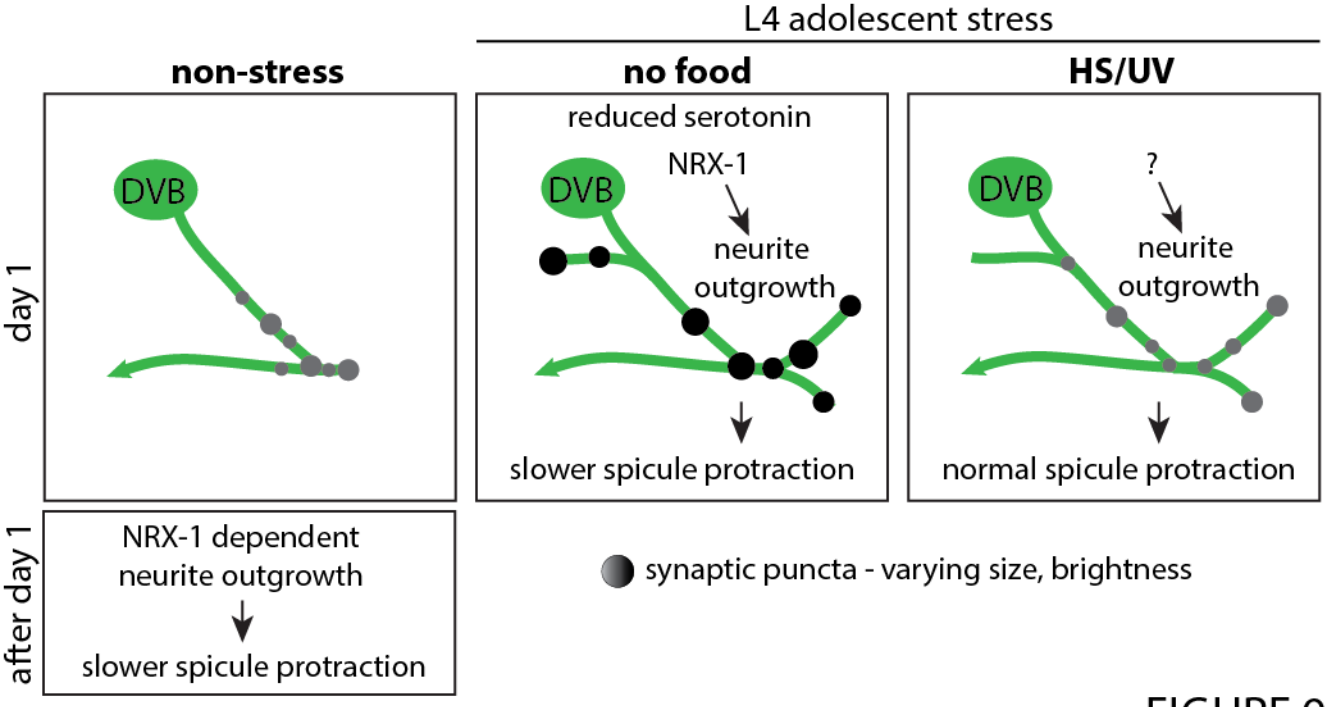
L4 adolescent stress
non-stress
no food
HS/UV
day 1
DVB
reduced serotonin
NRX-1
neurite outgrowth
slower spicule protraction
?
normal spicule protraction
after day 1
NRX-1 dependent neurite outgrowth
slower spicule protraction
synaptic puncta - varying size, brightness

FIGURE 9

Table 1. Strain table

Fig	Strain	mutant background	Array	DNA on array
1	OH15098	*him-8(e1489)*	*otls525*	*lim-6int4::gfp*
3	OH15099	*him-5(e1490)*	*otls541*	*lim-6^{int4}::wCherry*
			otls659	*lim-6int4::gfp::rab-3; ttx-3::gfp*
4	UP3805	*tph-1(n4662); him-8(e1489)*	*otls525*	*see above*
5	OH15111	*unc-119(ed3); nrx-1(wy778[unc-119(+)]); him-8(e1489)*	*otls525*	*see above*
5	OH15116	*nrx-1(gk246237); him-8(e1489)*	*otls525*	*see above*